The Role of Tryptophan Residues in an Integral Membrane Protein: Diacylglycerol Kinase†

Elizabeth H. Clark, J. Malcolm East, and Anthony G. Lee*

Division of Biochemistry and Molecular Biology, School of Biological Sciences, University of Southampton, Southampton SO16 7PX, United Kingdom

Received April 16, 2003; Revised Manuscript Received July 24, 2003

ABSTRACT: Tryptophan residues are thought to play special roles in integral membrane proteins, anchoring transmembrane α-helices into the lipid bilayer. We have studied the effect of mutating the five Trp residues in the diacylglycerol kinase (DGK) of *Escherichia coli* to Leu residues. The fluorescence emission maxima for DGK and a variety of Trp mutants in bilayers of dioleoylphosphatidylcholine [di(C18:1)PC] are all centered at ca. 327 nm, suggesting that all five Trp residues are located close to the glycerol backbone region of the bilayer. This is also consistent with fluorescence quenching experiments, measuring the separation between the Trp residues and the bromine atoms in a bilayer of dibromostearoylphosphatidylcholine. Mutation of Trp residues in DGK was found to have significant effects on activity for DGK reconstituted into bilayers of di(C18:1)PC containing 30 mol % 1,2-dihexanoylglycerol (DHG). Of the mutants containing a single Trp residue, only that containing Trp-112 was found to give active protein. The presence of both Trp-25 and Trp-112 gave higher activity than Trp-112 alone. Trp-25 and Trp-112 are the most important Trp residues in DGK as far as activity is concerned. Effects of mutations on K_m for DHG were generally greater than effects on v_{max}. The activity of wild-type and mutant DHGs reconstituted into bilayers of phosphatidylcholines was sensitive to the chain length of the phospholipid, with highest activities for chain lengths of C18 or C20 and lower activities in phosphatidylcholines with shorter or longer chains. Compared to wild-type DGK, the Trp mutants were less affected by long-chain phosphatidylcholines but more affected by short-chain phospholipids. In mutants lacking Trp-25, low activities in short-chain phospholipids followed from a decrease in v_{max} compared to wild type, combined with an increase in K_m value for DHG, as observed in the wild type. It is suggested that Trp-25 plays a role in maintaining the alignment of ATP and DHG at the active site. Fluorescence emission spectra for the Trp mutants do not change significantly with changing fatty acyl chain length from C14 to C24, showing efficient hydrophobic matching between DGK and the surrounding lipid bilayer. It is suggested that hydrophobic matching is achieved by tilting of the transmembrane α-helix or rotation of residues at the ends of the helices about the Cα−Cβ bond linking the residue to the helix backbone. As well as any structural effects, the presence of Trp residues in DGK has a clear effect on thermal stability.

Although about 25% of sequenced genes code for membrane proteins, only about 30 unique structures of integral membrane proteins have been solved to atomic resolution, compared to about 3000 unique structures for water-soluble proteins. Further, even when a high-resolution crystal structure is available, it is often unclear how the protein sits in the lipid bilayer that surrounds it in the membrane, because very few lipid molecules are resolved in high-resolution structures of membrane proteins (*1*). Understanding how an integral membrane protein interacts with the surrounding lipid bilayer is important since lipids and proteins must have co-evolved to give functional membranes; the structure of the lipid bilayer must be compatible with proper function of the proteins in the membrane, and the membrane proteins must be compatible with the formation of a lipid bilayer that can serve as an efficient permeability barrier. There is therefore much room for indirect methods in the study of membrane proteins, both to provide information about the structure of the protein and to provide information about the location of the protein in the lipid bilayer.

Analysis of the distribution of amino acid residues in transmembrane α-helices has shown that the distribution of residues is highly nonrandom (*2*, *3*). Ends of transmembrane α-helices are often marked by the presence of Trp or Tyr residues, which have been suggested to act as "floats" at the interface between the hydrocarbon core of the lipid bilayer and the lipid headgroup region, serving to fix the helix within the lipid bilayer. A preference of Trp residues for the interface region of a lipid bilayer reflects the amphipathic nature of the Trp residue; Trp has the largest nonpolar surface of all the amino acids, but its NH group is capable of forming hydrogen bonds (*1*). The importance of Trp residues at the ends of transmembrane α-helices has been demonstrated in experiments using a glycosylation mapping technique to study the location of poly(Leu) helices within the lipid bilayer component of the membrane of the endoplasmic reticulum (*4*). Braun and von Heijne (*4*) showed that

† We thank the BBSRC for a studentship (to E.H.C.).

* To whom correspondence should be addressed. Phone 44 (0) 2380 594331. Fax: 44 (0) 2380 594459. E-mail: agl@soton.ac.uk.

10.1021/bi034607e CCC: $25.00
Published on Web 08/27/2003

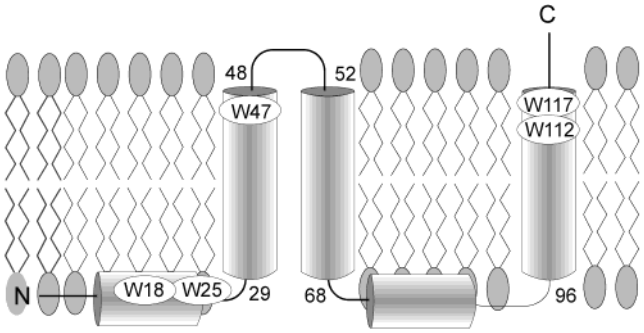

FIGURE 1: Predicted structure of DGK showing the positions of the five Trp residues.

the presence of a Trp residue in the polar region flanking the hydrophobic stretch of Leu residues pushed the helix into the membrane and a Trp residue in the hydrophobic region close to the end of the helix pulled the helix out of the membrane.

The location of Trp residues at the ends of transmembrane α-helices is particularly fortunate for studies of membrane protein structure since fluorescence emission spectra of Trp residues are very sensitive to environment (*5*) so that any changes in the location of a Trp residue with respect to the bilayer interface would be expected to lead to significant changes in fluorescence emission spectra. Here we show how Trp fluorescence emission spectra can be used to study the structure of diacylglycerol kinase (DGK)[1] of *Escherichia coli* in a membrane environment and how study of Trp mutants of DGK can provide information about the role of Trp residues in the function of an integral membrane protein. DGK catalyzes the reaction

$$\text{diacylglycerol} + \text{ATP} \leftrightharpoons \text{phosphatidic acid} + \text{ADP}$$

and is highly suitable for the proposed studies, for a number of reasons. DGK shows simple Michaelis−Menten kinetics with respect to both ATP and diacylglycerol, the mechanism involving direct phosphoryl transfer from ATP to diacylglycerol (*6*, *7*). It is the smallest known kinase and is predicted to contain three transmembrane α-helices with two amphipathic helices on the cytoplasmic side of the membrane (Figure 1), in a homotrimeric structure with three active sites per trimer, the active sites being at subunit−subunit interfaces (*8*, *9*). Finally, we have shown that it can be reconstituted into lipid bilayers of defined composition and that its activity depends on the structure of the surrounding phospholipids (*10*, *11*).

MATERIALS AND METHODS

Materials and General Procedures. Dimyristoleoylphosphatidylcholine [di(C14:1)PC], dipalmitoleoylphosphatidylcholine [di(C16:1)PC], dioleoylphosphatidylcholine [di(C18:1)PC], dieicosenoylphosphatidylcholine [di(C20:1)-PC], dierucoylphosphatidylcholine [di(C22:1)PC], dinervonylphosphatidylcholine [di(C24:1)PC], and 1,2-dioleoylglycerol (DOG) were obtained from Avanti Polar Lipids. Potassium cholate was purified by dissolving equimolar quantities of cholic acid and potassium hydroxide in methanol, followed by precipitation with excess diethyl ether. 1,2-Dihexanoylglycerol (DHG) was synthesized from 3-benzylglycerol and caproic acid following the method used by Czerski and Sanders (*12*) for the synthesis of dibutyrylglycerol. Phospholipids were brominated as described in East and Lee (*13*) to give brominated analogues dibromomyristoylphosphatidylcholine [di(Br_2C14:0)PC], dibromostearoylphosphatidylcholine [di(Br_2C18:0)PC], and dibromolignoceroylphosphatidylcholine [di(Br_2C24:0)PC].

A plasmid expressing His-tagged DGK was generously provided by Professor James Bowie of UCLA. DGK was purified as described in Pilot et al. (*10*). Concentrations of protein were estimated using an extinction coefficient of 30800 M^{-1} cm^{-1} at 280 nm for wild-type DGK, reducing the extinction coefficient for mutant DGKs by 5600 M^{-1} cm^{-1} for each Trp residue removed. Purified DGK was reconstituted into lipid bilayers by mixing lipid and DGK in cholate followed by dilution to decrease the concentration of cholate below its critical micelle concentration (*10*). For activity measurements, DHG at the required concentration was included with the phospholipid at the reconstitution stage. DGK activity was measured using a coupled enzyme assay (*10*). The assay medium consisted of buffer (60 mM Pipes, pH 6.9) containing phosphoenolpyruvate (2 mM), NADH (0.2 mM), ATP (5 mM), Mg^{2+} (20 mM), pyruvate kinase (18 units), and lactate dehydrogenase (22 units). The mixture was incubated at 25 °C for 10 min to ensure that any residual ADP in the ATP sample was consumed. The assay was initiated by addition of DGK (1.5 μg) to 1 mL of the assay medium, and the oxidation of NADH was monitored by the decrease in absorbance at 340 nm.

Fluorescence Measurements. For fluorescence measurements 120 μL of the lipid/protein mixture in cholate was diluted into 3 mL of buffer (60 mM Pipes, 1 mM EGTA, pH 6.9) and the fluorescence recorded on an SLM 8000C fluorometer with excitation at 290 nm. To obtain accurate values for wavelengths of maximum fluorescence emission intensity (λ_{max}) and spectral widths (ω_λ), fluorescence spectra were fitted to skewed Gaussian curves

$$F = F_{max} \exp\{-(\ln 2)[\ln(1 + 2b(\lambda - \lambda_{max})/\omega_\lambda)/b]^2\} \quad (1)$$

where F and F_{max} are the fluorescence intensities at wavelengths λ and λ_{max}, respectively, b is the skew parameter, and ω_λ is the peak width at half-height (*14*). The emission maximum for a solution of indole in ethanol was 322.8 nm on the fluorometer used for these studies. For acrylamide quenching experiments an excitation wavelength of 295 nm was used to minimize the inner filter effect, which was corrected for using the factor of $10^{\epsilon c 0.5}$ where ϵ is the extinction coefficient for acrylamide at 295 nm and c is the concentration of acrylamide (*5*).

Circular Dichroism. Spectra were recorded on a Jasco J-720 cicular dichroism spectrometer. The protein concentration was 1 mg/mL, and spectra were recorded with a path length of 0.01 cm at 25 °C. The spectra are the average of nine scans and were corrected for background by subtraction.

[1] Abbreviations: DGK, diacylglycerol kinase; di(C14:1)PC, dimyristoleoylphosphatidylcholine; di(C16:1)PC, dipalmitoleoylphosphatidylcholine; di(C18:1)PC, dioleoylphosphatidylcholine; di(C20:1)PC, dieicosenoylphosphatidylcholine; di(C22:1)PC, dierucoylphosphatidylcholine; di(C24:1)PC, dinervonylphosphatidylcholine; DHG, 1,2-dihexanoylglycerol; DOG, 1,2-dioleoylglycerol; di(Br_2C14:0)PC, dibromomyristoylphosphatidylcholine; di(Br_2C18:0)PC, dibromostearoylphosphatidylcholine; di(Br_2C24:0)PC, dibromolignoceroylphosphatidylcholine; CD, circular dichroism.

Table 1: Activities of Mutant DGKs in Di(C18:1)PC

mutant	Trp residues present[a] 18	25	47	112	117	activity[b] (μmol min^{-1} mg^{-1})	v_{max}[c] (μmol min^{-1} mg^{-1})	K_m[c] (mol %), DHG
WT	x	x	x	x	x	102 ± 2	126 ± 7	6.0 ± 1.1
W18L		x	x	x	x	61 ± 6	78 ± 4	7.8 ± 1.2
W25L	x		x	x	x	23 ± 1	62 ± 12	50.3 ± 14.3
W18,25L			x	x	x	42 ± 1	82 ± 7	28.0 ± 4.2
W112,117				x	x	26 ± 3	89 ± 11	73.7 ± 12.2
W25,112		x		x		77 ± 3	115 ± 5.0	14.1 ± 1.3
W112				x		36 ± 3	91 ± 8	46.4 ± 7.5
W18	x					0		
W25		x				0		
W47			x			0		
W117					x	0		

[a] Trp residues present are marked with an x. [b] Activities measured at 30 mol % DHG and 5 mM ATP at 25 °C for DGK reconstituted into bilayers of di(C18:1)PC. [c] Values obtained by fitting the data in Figure 3.

Construction of Trp Mutants. The codons for Trp-18, Trp-25, Trp-47, and Trp-117 in the wild-type gene were replaced one by one with the Leu codon using the polymerase chain reaction to prepare oligonucleotide cassettes encoding Leu residues at the targeted positions. Cassettes were ligated into plasmid pSD005, a pTrcHisB plasmid containing the synthetic gene coding for the wild-type DGK (*8*). For Trp-18, Trp-25, Trp-47, and Trp-117 regions between the *Nco*I and *Stu*I sites, the *Stu*I and *Xho*I sites, the *Stu*I and *Aat*II sites, and the *Hin*dIII and *Pst*I sites, respectively, were replaced. The position of Trp-112 in relation to the available restriction sites meant that this residue could not be removed by use of a simple cassette. Instead, the recombinant PCR method was used to replace this residue using primers 5′-CATGGGTTCTGCAGCTGTTC-3′, 5′-GTTGCTGTTATCACCCTGTGCATCCTGCTGCTG-3′, 5′-CCGCCAAAACAGCCAAG-3′, and 5′-CAGCAGCAGGATGCACAGGGTGATAACAGCAAC-3′; mutations are underlined. Having removed all five Trp residues from the DGK gene, individual Trp residues were inserted back into the gene using oligonucleotide cassettes. Altered plasmids were sequenced to verify the correct mutation before transformation into *E. coli* strain Top10 for expression and purification as described (*10*).

Thermal Inactivation. DGK reconstituted in di(C18:1)PC containing 30 mol % DHG at a molar ratio of total lipid:DGK of 6000:1 was incubated at 75 °C in 60 mM Pipes and 1 mM EGTA, pH 6.9. Aliquots were removed at the appropriate times, and their activities were determined.

RESULTS

Expression of Mutants. Mutants prepared are listed in Table 1. Mutants with single substitutions at the Trp-18 and Trp-25 positions are denoted W18L and W25L, respectively, and the mutant with a double substitution of Trp-18 and Trp-25 is denoted W18,25L. Five mutants containing single Trp residues were prepared and are denoted W18, W25, W47, W112, and W117. Two mutants containing pairs of Trp residues were also prepared and are denoted W25,112 and W112,117. All expressed in *E. coli* at comparable levels except for the single Trp mutants W18, W25, W47, and W117, which expressed at ca. 10−20% of wild-type levels. Lau and Bowie (*15*) reported that the mutants W25L,W117R and W112F,W117R could only be purified in low amounts and were prone to aggregation.

Circular dichroism (CD) spectra of DGK and its mutants were recorded in dodecyl maltoside. As shown in Figure 2

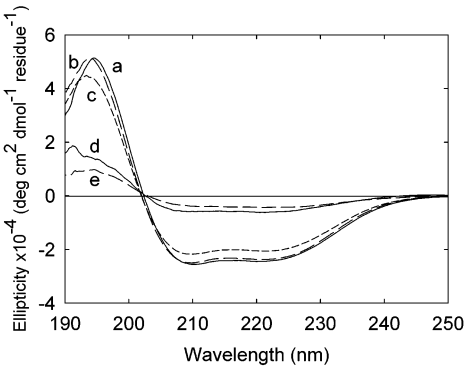

FIGURE 2: Circular dichroism spectra of wild-type and mutant DGKs in dodecyl maltoside. The samples contained 1 mg/mL DGK in 10 mM sodium phosphate, 100 mM NaCl, pH 7.5, and 0.5% dodecyl maltoside. The spectra are as follows: (a, solid line) wild type; (b, long dashed line) W25,112; (c, short dashed line) W112; (d, solid line) W25; (e, long dashed line) W47.

the shape of the CD spectrum for wild-type DGK was typical for that of a protein with a high α-helical content. CD spectra for W25,112 and W112 were very similar to that of wild type (Figure 2), as were the CD spectra of W18L, W25L, W18,25L, and W112,W117 (data not shown). However, spectra for W25 and W47 were much reduced in intensity, suggesting that these mutants were largely aggregated and not contributing to the observed spectrum.

Activities of Mutant DGKs. DGK was reconstituted into bilayers of di(C18:1)PC, and the activity was assayed at 30 mol % DHG in the membrane, at an ATP concentration of 5 mM. As shown in Table 1, the activity of W18L was 61% of the wild-type activity whereas the activity of W25L was only 23% of wild type. The activity of the double mutant W18,25L was about double that of W25L (Table 1). Lau and Bowie (*15*) reported that the double mutant W18,25L was more stable than the single mutant W25L. The mutants W18, W25, W47, and W117 containing single Trp residues showed no activity whereas W112 showed an activity about one-third of that of the wild type. The activity of W112,117 was comparable to that of W112, but the activity of W25,-112 was about 75% of wild-type activity. Thus the presence of Trp-112 is essential for activity, and the presence of Trp-25 leads to higher activity. Activities of the mutants in bilayers of di(C18:1)PC were studied as a function of mole percent DHG in the bilayer (Figure 3). The data all fit to the Michaelis−Menten equation with the values for K_m and v_{max} given in Table 1. Activities of all mutants except for

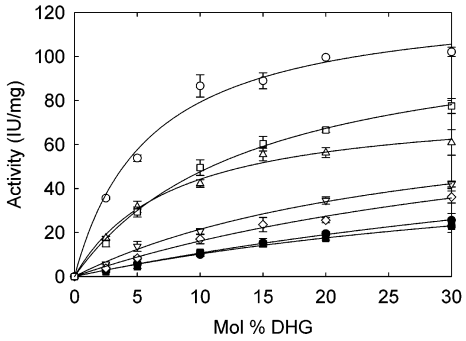

FIGURE 3: Activity of mutant DGKs reconstituted in di(C18:1)-PC. DGK was reconstituted with di(C18:1)PC at a total lipid:DGK molar ratio of 6000:1 and the given mole fraction of DHG. Activities were measured at 25 °C with 5 mM MgATP. Mutants were as follows: (○) WT; (□) W25,112; (△) W18L; (▽) W18,25L; (◇) W112; (●) W112,117; (■) W25L. The solid lines show fits to the Michaelis−Menten equation with the values for K_m and v_{max} given in Table 1.

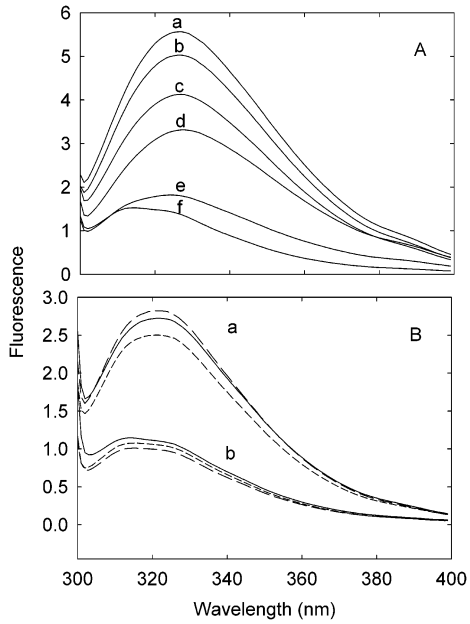

FIGURE 4: Fluorescence emission spectra for DGK. (A) Fluorescence emission spectra are shown for wild-type and mutant DGKs reconstituted into di(C18:1)PC. Samples were as follows: (a) wild-type DGK; (b) W18L; (c) W25L; (d) W18,25L; (e) W112,117; (f) W112. (B) Fluorescence emission spectra are shown for W25,112 (a) and W112 (b) reconstituted into phosphatidylcholines with chain lengths of (solid line) C14, (long dash) C18, and (short dash) C24. The concentration of DGK was 2 μM, and the molar ratio of lipid to DGK was 100:1. The buffer was 60 mM Pipes, pH 6.9, and fluorescence was excited at 290 nm.

W18L were very low when assayed in octyl glucoside micelles with dioleoylglycerol as substrate (data not shown).

Fluorescence Emission Spectra for Wild-Type and Mutant DGK. Fluorescence emission spectra for wild-type and mutant DGKs reconstituted into di(C18:1)PC are shown in Figure 4. All of the mutants containing three or more Trp residues show fluorescence emission spectra for Trp centered around 327 nm, typical for Trp residues in a hydrophobic environment. For the active mutants containing one or two Trp residues (Trp-25, Trp-112, and Trp-117), emission spectra were centered at slightly shorter wavelengths (Table 2), suggesting a somewhat more hydrophobic environment for these Trp residues, particularly for Trp-112.

Spectra were excited at 290 nm to reduce the magnitude of the light scatter observed at wavelengths close to 300 nm. Using an excitation wavelength of 295 nm to reduce excitation of the two Tyr residues in DGK had no significant effect on the emission spectra. For example, for wild-type DGK the emission maximum observed with excitation at 295 nm was 326.3 ± 0.05 nm compared to 326.5 ± 0.1 nm with excitation at 290 nm.

Lodokhin et al. (*16*) have shown that the relationship between the wavelength of maximum emission and the width of the fluorescence emission spectrum measured at half-maximum peak height depends on the nature of the environment of the Trp residues in a protein and on the heterogeneity of the environment. For a single Trp residue shielded from water, fluorescence emission centered at ca. 327 nm would be expected to show a spectrum of width ca. 50 nm. For wild-type DGK and for the mutants in di(C18:1)PC the spectral widths are ca. 50 nm, again suggesting a rather similar, hydrophobic environment for all of the Trp residues in DGK (Table 2).

Removal of Trp-18 results in a smaller decrease in fluorescence intensity than that seen on subsequent removal of Trp-25 (Figure 4A). The decrease in fluorescence intensity on removal of Trp-47 is comparable to that on removal of Trp-25 and is comparable to the fluorescence intensity of W112. By difference, the fluorescence intensity of Trp-117 is comparable to that of Trp-18. These results suggest that Trp-18 and Trp-117 could be located in more exposed, less hydrophobic environments than the other Trp residues.

Quenching of fluorescence is seen on reconstitution into bilayers of di(Br_2C18:0)PC (Table 2). Levels of quenching for all of the active mutants are comparable and similar to that seen with wild-type DGK, suggesting that locations of all of the Trp residues relative to the bromine atoms in di-(Br_2C18:0)PC are similar. This is also consistent with the observation that quenching results in no significant shifts in emission spectra, as shown in Figure 5 for wild-type DGK; if wild-type DGK contained Trp residues at a variety of positions within the lipid bilayer, selective quenching of the deeper Trp residues by di(Br_2C18:0)PC would have led to a significant shift of the spectrum to longer wavelengths (*17*), and this is not seen.

Trp fluorescence in DGK is also quenched by the water-soluble quencher acrylamide. The level of quenching increases linearly with increasing concentrations of acrylamide up to 0.24 M (data not shown). Levels of quenching for wild-type and mutant DGKs observed with 0.24 M acrylamide are similar (Table 2), again consistent with a similar environment for all of the Trp residues. Quenching with acrylamide results in no significant changes in the wavelength of maximum emission or the peak width at half-height, values for wild-type DGK being 325.6 ± 0.04 nm and 50.4 ± 0.1 nm, respectively, in the presence of 0.24 M acrylamide, not significantly different from the values in the absence of acrylamide (Table 2). The absence of an acrylamide-induced shift to shorter wavelength is consistent with an absence of depth heterogeneity for the Trp residues in DGK.

Bolen and Holloway (*18*) studied the quenching of a Trp-containing peptide by phospholipids containing one nonbrominated and one dibrominated fatty acyl chain and showed that the extent of quenching fitted to a model with a sixth power dependence of quenching efficiency on separation

Table 2: Fluorescence Properties of Wild-Type and Mutant DGKs in Di(C18:1)PC and Di(Br_2C18:0)PC

mutant	λ_{max} (nm) in di(C18:1)PC[a]	ω_λ (nm) in di(C18:1)PC[a]	F/F_0 in di(Br_2C18:0)PC[b]	h (Å)[c]	F/F_0, acrylamide[d]
WT	326.5 ± 0.1	49.8 ± 0.3	0.21	7.9	0.80 ± 0.01
W18L	326.5 ± 0.1	49.8 ± 0.3	0.17	7.2	0.80 ± 0.02
W25L	327.0 ± 0.2	50.8 ± 0.4	0.28	8.8	0.75 ± 0.01
W18,25L	328.1 ± 0.2	51.2 ± 0.6	0.22	8.0	0.80 ± 0.03
W112,117	323.2 ± 0.3	50.6 ± 0.7	0.25	8.5	0.83 ± 0.01
W25,112	321.1 ± 0.3	48.8 ± 0.7	0.23	8.2	0.82 ± 0.01
W112	319.7 ± 0.3	47.2 ± 0.9	0.30	9.0	0.85 ± 0.01

[a] Wavelengths of maximum fluorescence emission intensity (λ_{max}) and spectral widths (ω_λ) were obtained by fitting fluorescence spectra recorded in di(C18:1)PC to eq 1 for a skewed Gaussian. [b] F_0 and F are fluorescence intensities for DGK reconstituted into di(C18:1)PC and di(Br_2C18:0)PC, respectively. [c] h is the separation between the Trp residues and the bromine atoms in di(Br_2C18:0)PC calculated using the equations of Koppel et al. (*20*). [d] F_0 and F are fluorescence intensities for DGK reconstituted into di(C18:1)PC in the absence and presence of 0.24 M acrylamide, respectively.

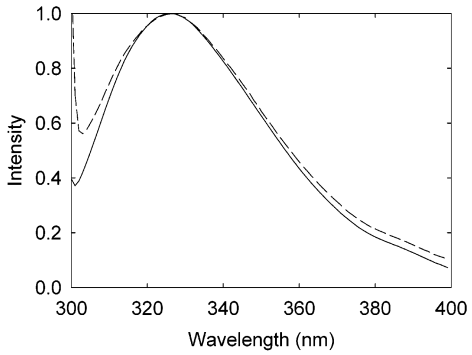

FIGURE 5: Fluorescence emission spectra for wild-type DGK. Fluorescence emission spectra are shown for wild-type DGK reconstituted into di(C18:1)PC (solid line) and di(Br_2C18:0)PC (broken line). The concentration of DGK was 2 μM, and the molar ratio of lipid to DGK was 100:1. The buffer was 60 mM Pipes, pH 6.9, and fluorescence was excited at 290 nm. Spectra have been normalized to 1 at λ_{max}.

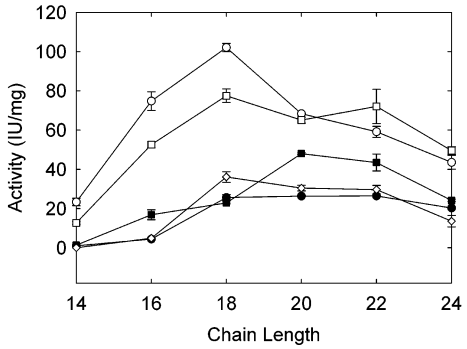

FIGURE 6: Activity of mutant DGKs as a function of phospholipid fatty acyl chain length. DGK was reconstituted into bilayers of phosphatidylcholines with monounsaturated fatty acyl chains of the given chain length at a total lipid:DGK molar ratio of 6000:1 and 30 mol % mole fraction of DHG. Activities were measured at 25 °C with 5 mM MgATP. Mutants were as follows: (○) WT; (□) W25,112; (◇) W112; (●) W112,117; (■) W25L.

distance. This does not, of course, prove that the quenching mechanism is resonance energy transfer. Indeed, Ladokhin (*19*) has shown that these same data can be interpreted in terms of a collisional model for quenching when account is taken of the depth distributions of the fluorophore and quencher in the membrane. Nevertheless, the observation that the experimental data fit reasonably well to an R^6 curve suggests that an analysis in these terms can be used to estimate separation distances in our experiments. A convenient analysis of resonance energy transfer in a membrane system is that of Koppel et al. (*20*), who treated the fluorophors and quenchers as being distributed randomly on two planes a distance h apart. Fluorescence quenching can then be represented by the equation:

$$\frac{F_0}{F_0 - F} = 1 + \sigma^{-1.1}\left[\frac{0.62}{\pi R_o^{\,2}}\exp(-0.34r + 1.63r^2)\right]^{1.1} \quad (2)$$

where r is defined as

$$r = h/R_o \quad (3)$$

and σ is the surface density of dibrominated fatty acyl chains. Bolen and Holloway (*18*) estimated a value for R_o in eq 2 of 9.25 Å but did not take into account the fact that quenching of the Trp residue, located in the middle of the lipid bilayer, could take place from both monolayers (*21*). Refitting the data of Bolen and Holloway (*18*) to eq 2 using a concentration of brominated chains of 1 per 35 Å^2 to account for quenching from both monolayers gives a value for R_o of 7.8 Å, in good agreement with the value of 8.2 Å estimated by Mall et al. (*22*) from studies of the quenching of Trp fluorescence by dibromotyrosine. Using the value of 7.8 Å for R_o and an area per chain of 35 Å^2 for phospholipids containing two dibrominated fatty acyl chains and a surface area of 1400 Å^2 for a DGK trimer, the observed levels of quenching for DGK give the separations listed in Table 2. The limitations of an analysis of fluorescence quenching using a single fluorescence quencher have been discussed by Ladhokin (*19*), but the estimated separation distances agree well with the suggested location for the Trp residues in DGK. The hydrophobic thickness of a bilayer of di(C18:1)PC, defined by the positions of the glycerol backbones, is about 27 Å (*23*), and since the bromine atoms in di(Br_2C18:0)PC are at the C9 and C10 positions, the bromine atoms will be about 7 Å from the glycerol backbone region of the bilayer. Thus all of the Trp residues in DGK are likely to be located close to the glycerol backbone region (Table 2).

Effects of Chain Length on Activity. Activities were measured for the mutant DGKs reconstituted into bilayers of phosphatidylcholines containing monounsaturated fatty acyl chains of lengths between C14 and C24. As reported previously (*10*), the activity of wild-type DGK is highest in bilayers of di(C18:1)PC, and activities are lower in phosphatidycholines with either shorter or longer fatty acyl chains (Figure 6). The chain length dependence of the activity of W25,112 is similar to that of wild type with a gradual decrease in activity with decreasing chain length below C18 but with a smaller decrease in activity with increasing chain length beyond C18 than seen with wild type. W112 and

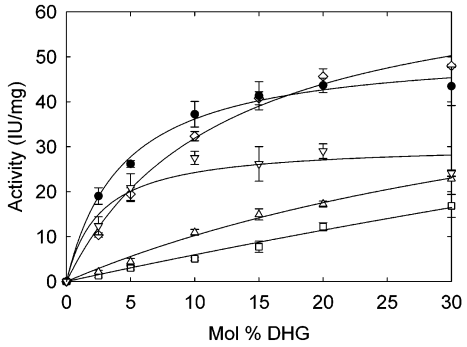

FIGURE 7: Effects of phosphatidylcholine chain length on the activity of W25L. W25L was reconstituted at a total lipid:DGK molar ratio of 6000:1 and the given mole fraction of DHG in phosphatidylcholines with monounsaturated chains of lengths (□) C16, (△) C18, (◇) C20, (●) C22, and (▽) C24. Activities were measured at 25 °C with 5 mM MgATP. The solid lines show fits to the Michaelis−Menten equation with the values for K_m and υ_{max} plotted in Figure 8.

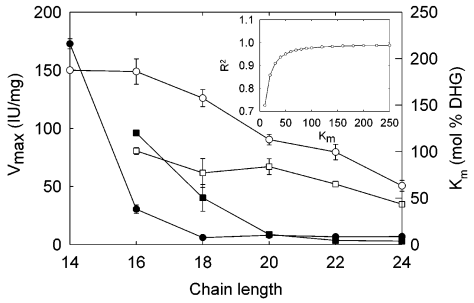

FIGURE 8: Effects of phosphatidylcholine chain length on K_m and υ_{max} values for wild-type DGK and W25L. K_m (●, ■) and υ_{max} (○, □) values obtained from fits of rates vs the mole fraction of DHG at an ATP concentration of 5 mM are plotted vs chain length for wild-type DGK (○, ●) and W25L (□, ■). Insert: for W25L in di(C16:1)PC, a lower limit for the K_m value of ca. 120 mol % DHG was determined from plots of the coefficient of determination of the fit (R^2) to the experimental data for the given values for K_m with υ_{max} as a variable. The value for K_m for wild-type DGK in di(C14:1)PC was obtained in a similar way, assuming the same value for υ_{max} as in di(C16:1)PC, as described in the text.

W112,117 show more sensitivity to short-chain lipids than wild-type DGK, with very low activities in di(C16:1)PC and no measurable activity in di(C14:1)PC. As with W25,112, the activities of W112 and W112,117 vary little with increasing chain length beyond C18 (Figure 6). The chain length optimum for W25L has shifted to C20 (Figure 6).

Activities for W25L as a function of mole percent DHG are shown in Figure 7. The data all fit to the Michaelis−Menten equation with the values for K_m and υ_{max} given in Figure 8. For W25L in di(C16:1)PC there was insufficient curvature in the plots to obtain reliable values for K_m and υ_{max}. A lower limit for K_m was therefore estimated from a plot of the coefficient of determination of the fit (R^2) to the experimental data for fixed values for K_m with υ_{max} as a variable (Figure 8). In this way a minimum value for the K_m for DHG was estimated as 120 mol % DHG with a corresponding minimum value for υ_{max} of 80.6 ± 2.9 IU/mg. This value for υ_{max} is, within experimental error, the same as those for W25L in di(C18:1)PC and di(C20:1)PC. Data for the activity of wild-type DGK as a function of mole percent DHG (data not shown) were fitted in the same way to give the values for K_m with υ_{max} plotted in Figure 8. In this case the curvature on the plots of activity in di(C14:1)-PC vs mole percent DHG were insufficient to obtain reliable values for K_m and υ_{max}, and the data were therefore fitted assuming a value for υ_{max} in di(C14:1)PC equal to that in di(C16:1)PC. The reason for the lower activities for W25L than wild-type DGK are predominantly a large increase in K_m value for DHG combined with a smaller decrease in υ_{max} value.

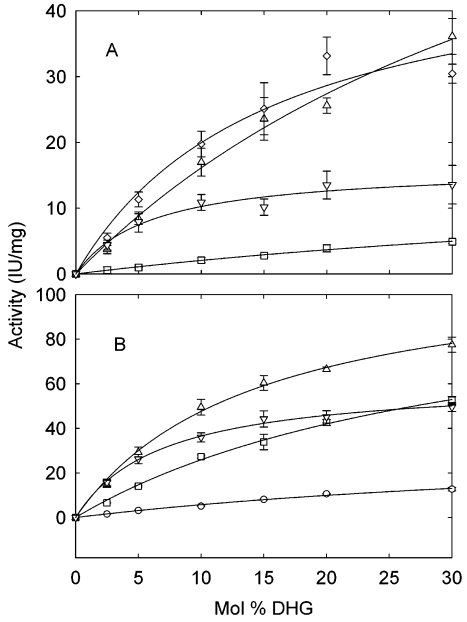

FIGURE 9: Effects of phosphatidylcholine chain length on the activity of W112 and W25,112. W112 (A) and W25,112 (B) were reconstituted at a total lipid:DGK molar ratio of 6000:1 and the given mole fraction of DHG in phosphatidylcholines with monounsaturated chains of lengths (○) C14, (□) C16, (△) C18, (◇) C20, and (▽) C24. Activities were measured at 25 °C with 5 mM MgATP. The solid lines show fits to the Michaelis−Menten equation with the values for K_m and υ_{max} plotted in Figure 10.

Activities for W112 and W25,112 as a function of mole percent DHG are shown in Figure 9 with the derived values for K_m and υ_{max} in Figure 10. For W112 the small dependence of activity on fatty acyl chain length between C18 and C24 shown in Figure 6 is due to an decrease in υ_{max} with increasing chain length, offset by an decrease in K_m (Figure 10). The decrease in K_m with increasing chain length for W112 is comparable to that seen for W25L (Figure 8). The marked decrease in activity in di(C16:1)PC follows from a large decrease in υ_{max}, and presumably, an even lower υ_{max} in di(C14:1)PC explains the lack of activity measurable in di(C14:1)PC. The higher activities observed for W25,112 than for W112 follow both from a higher υ_{max} and from a lower K_m value. For chain lengths of C18 or longer, K_m and υ_{max} values for W25,112 are very similar to wild-type values, and the lower activities observed for W25,112 in shorter chain lipids are due to a decrease in υ_{max} value mirroring that seen in W112 but occurring at C14 rather than C16.

Effects of Chain Lengths on Fluorescence Emission Spectra. Any significant movement of the Trp residues in DGK with respect to the bilayer−water interface resulting from changes in bilayer thickness would be expected to be reflected in changes in the fluorescence emission spectra for the Trp residues. Fluorescence emission spectra for W25,112 and W112 show no significant differences when reconstituted in bilayers of di(C14:1)PC, di(C18:1)PC, or di-(C24:1)PC (Figure 4B).

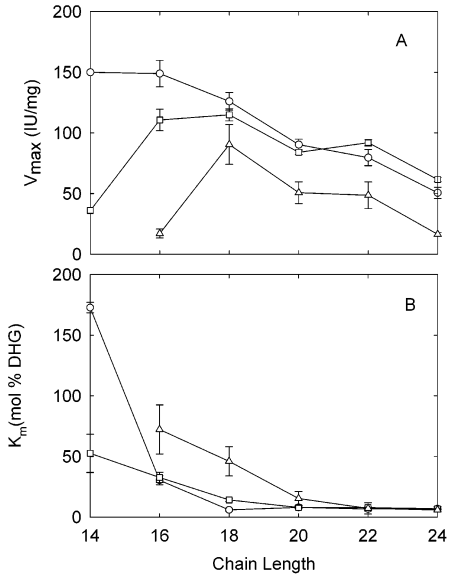

FIGURE 10: Effects of phosphatidylcholine chain length on v_{max} (A) and K_m (B) values for W112 and W25,112. Values of v_{max} (A) and K_m (B) were obtained from fits of rates vs the mole fraction of DHG at an ATP concentration of 5 mM are plotted vs chain length for wild-type DGK (○), W112 (△), and W25,112 (□).

Table 3: Effects of Fatty Acyl Chain Length on Fluorescence Quenching of Wild-Type and Mutant DGKs

	fatty acyl chain length[a]					
	C14		C18		C24	
mutant	F/F_0	h (Å)	F/F_0	h (Å)	F/F_0	h (Å)
wild type	0.24	8.3	0.21	7.9	0.51	10.7
W112	0.24	8.3	0.30	9.0	0.44	10.2
W25,112	0.20	7.8	0.23	8.2	0.46	10.3

[a] F_0 and F are fluorescence intensities for DGK reconstituted into nonbrominated and brominated phosphatidylcholines of the given chain lengths, and h is the separation between the Trp residues and the bromine atoms calculated using the equations of Koppel et al. (*20*). For the C14 and C18 chains, the bromine atoms are at the 9,10 positions whereas in the C24 chain the bromine atoms are at the 15,16 positions.

Levels of fluorescence quenching for wild-type DGK and the mutants W112 and W25,112 in di(Br_2C14:0)PC, di(Br_2-C18:0)PC, and di(Br_2C24:0)PC are compared in Table 3, together with estimates of the separation between the Trp residues and the bromine atoms, made using the equations of Koppel et al. (*20*). The bromine atoms are at the 15,16 positions of the fatty acyl chains in di(Br_2C24:0)PC and at the 9,10 positions in di(Br_2C14:0)PC and di(Br_2C18:0)PC. Thus the bromine atoms are ca. 12 Å from the glycerol backbone region in di(Br_2C24:0)PC, compared to 7 Å in the other lipids. Thus the increased Trp−bromine separation distance seen in di(Br_2C24:0)PC (Table 3) can be attributed to the deeper position of the bromine atoms in the bilayer.

Effects of Trp Residues on Thermal Stability. Lau et al. (*24*) have shown that changing single amino acids in DGK can have a significant effect on the thermal stability. The thermal inactivation kinetics of wild-type DGK and of the mutants W25L, W25,112, and W112 at 75 °C are shown in Figure 11. All of the data fitted well to a first-order rate equation. Mutation of Trp residues leads to reduced thermal stability; the times for half-inactivation decrease from 49 min for wild-type DGK, to 39 min for W25L, 28 min for W25,-112, and 23 min for W25.

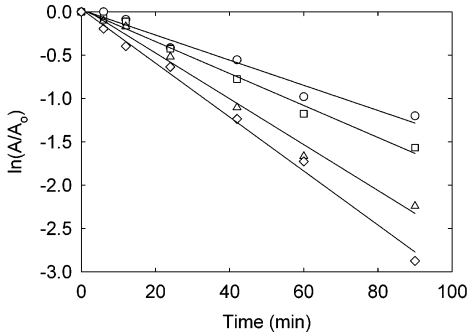

FIGURE 11: Thermal inactivation of wild-type and mutant DGKs at 75 °C. Data are shown for (○) wild-type DGK, (□) W25L, (△) W25,112, and (◇) W112. The lines show linear least-squares fits to the data.

DISCUSSION

Trp residues are often found at the ends of transmembrane α-helices in membrane proteins and have been suggested to play a special role in anchoring the helices into the membrane (*1*−*3*). DGK is predicted to contain three transmembrane α-helices (Figure 1) (*9*). Wen et al. (*25*) have suggested that transmembrane α-helix M1 is relatively short, containing just 14 hydrophobic residues, the N- and C-terminal ends of the helix being marked by Glu-34 and Asp-49, respectively, whereas M2 contains 17 hydrophobic residues flanked by Asp-51 and Glu-69, and M3 contains 22 hydrophobic residues flanked by Met-96 and Trp-117. In the family of bacterial DGKs, the residue equivalent to Glu-34 in *E. coli* DGK is not conserved, whereas Glu-28 is conserved in all but the DGK from the cyanobacterium *Synechocystis* sp. (*26*) where it is replaced by a Gln. If it is assumed that the N-terminal end of M1 is marked by Glu-28 rather than Glu-34, the length of transmembrane α-helix M1 becomes 21 residues. NMR studies of DGK in micelles suggest that residues 29−47 are helical (*27*), consistent with this suggestion. This would imply that Glu-34 is embedded within the lipid bilayer. There are precedents for suggesting that an acidic residue might be located within the hydrocarbon core of the bilayer. For example, in the Ca^{2+}-ATPase Asp-59 is buried within the bilayer and faces out into the bilayer, forming an ion pair with Arg-63 (*28*). It is possible that in *E. coli* DGK Glu-34 forms an ion pair with Arg-32. NMR studies of DGK in micelles suggest that transmembrane helix M2 starts at residue 52 (*27*). Wen et al. (*25*) also suggested that the bulk of the N-terminal region and the bulk of the region between transmembrane α-helices M1 and M2 formed amphipathic α-helices, as shown in Figure 1, and NMR studies of DGK in micelles are consistent with a helical structure for residues 18−25.

Effects of Mutation of Trp Residues on Production of DGK. None of the Trp residues are conserved in the family of bacterial DGKs, suggesting that none are located at the active site in DGK. It has been shown using random mutagenesis that all of the Trp resides can be substituted singly to give a protein showing at least 5% of wild-type activity (*25*). Generally, a wide range of substitutions is accepted, except for Trp-112 where only Cys and Gln were found to give active protein (*25*). In subsequent studies, a mutant DGK in which Trp-112 was replaced by Phe was found to be produced only at low levels and was unstable, as was a mutant in which Trp-25 was replaced by Leu, suggesting

some special role for these two Trp residues (*15*). Expression levels and levels of purified protein were low for all of the single Trp mutants except for W112. The CD spectrum for W112 in micelles of dodecyl maltoside was comparable to that of wild-type protein whereas the CD spectra of W25 and W47 were of low intensity, suggesting that most of the protein produced was aggregated and so did not contribute to the CD spectrum (Figure 2).

Location of Trp Residues in DGK in Relation to the Membrane. Fluorescence emission for all of the active Trp mutants of DGK reconstituted into bilayers of di(C18:1)PC occurs at low wavelengths, consistent with a hydrophobic environment for all of the Trp residues (Figure 4; Table 2). Fluorescence emission for the Trp residues in the potassium channel KcsA, which are located close to the glycerol backbone region of the bilayer, is centered at ca. 327 nm (*29*). Thus most of the Trp residues in DGK are also likely to be located close to the glycerol backbone region of the bilayer with, possibly, a deeper location for Trp-112 which has a more blue-shifted emission (Table 2). The similar half-height widths of all of the fluorescence emission spectra for DGK and similar levels of quenching by acrylamide are again consistent with a uniform environment for all of the Trp residues in DGK (Table 2). Finally, the levels of quenching of the Trp fluorescence in wild-type and mutant DGKs in di(Br_2C18:0)PC are very similar (Table 2), and using the equations of Koppel et al. (*20*), the separation between the plane containing the Trp residues and the plane containing the bromines is estimated to be ca. 7−9 Å (Table 2). The hydrophobic thickness of a bilayer of di(C18:1)PC is about 27 Å (*23*) so that the bromine atoms in di(Br_2C18:0)PC will be about 7 Å from the glycerol backbone region of the bilayer. This therefore is also consistent with all of the Trp residues in DGK being located close to the glycerol backbone region of the bilayer.

The extent of quenching observed with 0.24 M acrylamide (ca. 20%, Table 2) is less than might have been expected from studies of the quenching of the Trp fluorescence of model transmembrane α-helices in lipid bilayers where Caputo and London (*17*) observed quenching of ca. 40% for Trp residues at the ends of a transmembrane α-helix, similar to the level of quenching of the Trp residues in KcsA, which is ca. 37% (unpublished studies). The observation that the level of quenching is lowest for Trp-112 in DGK (Table 2) is consistent with a deeper location for Trp-112, as suggested above. The lower level of quenching than expected for wild-type DGK and the mutants containing three or four Trp residues suggests that these Trp residues could be shielded from collision with acrylamide by the amphipathic helices located on the cytoplasmic side of the membrane.

Effects of Trp Residues on the Function of DGK. Mutation of Trp residues in DGK has significant effects on the activity of the protein. The most critical Trp residues in DGK are Trp-25 and Trp-112. The only single Trp-containing mutant of DGK that shows activity is W112, for which υ_{max} is comparable to that of wild type although the K_m value for DHG is much increased (Table 1). The importance of W25 is shown by W25L where mutation of just Trp-25 results in a halving of υ_{max} and a large increase in K_m value for DHG (Table 1). The importance of Trp-25 is confirmed by the mutant W25,112, which has a value for υ_{max} comparable to that of wild type and a K_m value for DHG which is only double that for the wild type (Table 1). Effects of mutating the other Trp residues are much smaller. Interestingly, although mutation of Trp-18 results in a decrease in υ_{max}, mutation of both Trp-18 and Trp-25 results in a protein with a lower K_m than that for mutation of Trp-25 alone (Table 1). Thus the presence of Trp-18 in the absence of Trp-25 leads to a greater mislocation of the N-terminal amphipathic helix than seen in the absence of both Trp-18 and Trp-25. Similarly, the higher K_m value for W112,117 than for W112 suggests that the presence of Trp-117 leads to a worse packing of transmembrane α-helix M3 when Trp-112 is the only other Trp residue present in the protein. The lower K_m value for W18,25L than for W112,117 suggests that the presence of Trp-47 leads to improved packing of the helices.

Effects of mutations on K_m are much greater than those on υ_{max} except for mutation of Trp-18, which results in a 30% decrease in υ_{max} with no significant effect on K_m (Table 1). In contrast, mutation of Trp-25 results in an 8-fold increase in K_m with just a 2-fold decrease in υ_{max}. The low activities seen in the mutants W112,117 and W112 are largely due to a high K_m value, and in W25,112 the value for υ_{max} is close to the wild-type value, the lower activity than wild type following from a doubling of the K_m value for DHG. DGK catalyzes direct phosphoryl transfer from ATP to diacylglycerol (*6*), the binding site for ATP being at the subunit−subunit interfaces in the DGK trimer (*8*), suggesting that the DHG binding site could also be located at the subunit−subunit interfaces. The observed increases in K_m for DHG in the Trp mutants therefore suggest that packing at the subunit−subunit interfaces has changed as a result of the Trp mutations.

Effects of Changing Bilayer Thickness. Mutation of Trp residues in DGK has significant effects on how the activity of DGK depends on the chain lengths of the phospholipids surrounding DGK in the membrane. The activity of wild-type DGK is highest in bilayers of di(C18:1)PC and decreases with either increasing or decreasing chain length (*10*), as shown in Figure 6. Although effects are complex, it is clear that increasing chain length beyond C20 has much smaller effects on the activities of the mutants than decreasing chain length below C18. In the mutants W25L (Figure 8) and W112 (Figure 10), both lacking Trp-25, low activities in short-chain lipids follow from a decrease in υ_{max} compared to wild type, combined with an increase in K_m, which is also observed for wild-type DGK. The decrease in υ_{max} suggests that Trp-25 plays a role in maintaining the alignment of ATP and DHG on DGK to give a high rate of phosphoryl transfer, this role becoming important for fatty acyl chain lengths less than C20. The decrease in υ_{max} compared to wild type for W25,112 for chains shorter than C18 suggests that one or more of Trp-18, Trp-47, and Trp-117 also help to maintain the alignment of ATP and DHG at the active site, important for fatty acyl chain lengths below C16.

If the transmembrane α-helices contain 21 residues, they will be ca. 31.5 Å in length, assuming they form perfect α-helices for which the helix translation is 1.5 Å per residue. If the helices are untilted, then hydrophobic matching would be achieved with a bilayer of di(C20:1)PC for which the hydrophobic thickness is ca. 30.8 Å (*23*); if the helices in DGK are tilted with respect to the bilayer normal, then optimal matching would be to a slightly thinner bilayer. Highest activities for DGK are observed in bilayers of di-

(C18:1)PC or di(C20:1)PC (Figure 6), consistent with the proposed lengths of the transmembrane α-helices.

It is unlikely that any changes in fatty acyl chain length from that giving optimal matching will lead to exposure of hydrophobic regions of either the lipid bilayer or the protein to water, because the cost of exposing hydrophobic groups to water is high. As described above, the Trp residues in DGK appear to be located close to the glycerol backbone region in a bilayer of di(C18:1)PC. Any significant hydrophobic mismatch between DGK and the surrounding lipid bilayer as a result of changing the bilayer thickness would therefore be expected to lead to a significant change in the environment of the Trp residues in DGK. This would be detected as a change in wavelength of maximum fluorescence emission for the Trp, since the Trp emission spectrum is very environmentally sensitive (*5*). In fact, Trp emission spectra for W112 and W25,112 in di(C14:1)PC, di(C18:1)PC, and di(C24:1)PC are identical (Figure 4B), showing that hydrophobic matching between DGK and the surrounding lipid bilayer is very efficient, maintaining a constant environment for the Trp residues. This is confirmed by estimates of the separation between Trp residues and Br atoms for DGK reconstituted into bilayers of brominated phosphatidylcholines, which show that the Trp residues are located close to the glycerol backbone region in bilayers of chain lengths C14, C18, and C24 (Table 3).

Hydrophobic matching between DGK and the lipid bilayer could be achieved by distortion of the lipid bilayer or by distortion of DGK or by some combination of the two. Distortion of the lipid bilayer around a rigid DGK molecule would not be expected to lead to any change in activity for DGK. The fact that changes in activity for DGK are observed with changing fatty acyl chain length therefore suggests that hydrophobic matching involves at least some distortion of the DGK molecule. This is likely to be a tilting of the transmembrane α-helix or rotation of residues at the ends of the helices about the Cα−Cβ bond linking the residue to the helix backbone (*1*).

Role of Trp Residues in DGK. None of the five Trp residues are conserved in the family of bacterial DGKs, suggesting that none are located at the active site. However, all five are located close to the glycerol backbone region of the bilayer, suggesting that they could play a role in fixing the protein within the lipid bilayer. Of these five, Trp-25 and Trp-112 have the largest effects on activity. Wen et al. (*25*) showed that Ala-17 in the N-terminal amphipathic α-helix could not be substituted without loss of activity, suggesting that Ala-17 was part of the active site of the enzyme, so that the correct arrangement of the N-terminal amphipathic α-helix will be important for function. Mutation of Trp-25 leads to significant loss of activity (Table 1) so that Trp-25 could be important in localizing the N-terminal amphipathic α-helix correctly with respect to the membrane surface. Trp-47 is located at the C-terminal end of transmembrane α-helix M1, but transmembrane α-helices M1 and M2 are linked by the short linker ^{47}WLDVDA^{52}, and the presence of two charged residues in this sequence could well result in good localization of M1 even in the absence of Trp-47. However, the sequence from Trp-112 toward the end of transmembrane α-helix M3 to the C-terminus (^{112}WCILLWSHFG) is hydrophobic except for the His residue. The presence of the two Trp residues might therefore be important in locating M3 correctly within the bilayer. It is not obvious why of the two Trp residues in this region Trp-112 is essential whereas Trp-117 is not (Table 1).

As well as any structural effects, the presence of Trp residues in DGK has a clear effect on thermal stability, the half-time for inactivation at 75 °C decreasing from 49 min for wild-type DGK to 23 min for W112 (Figure 11). An important role for Trp residues in membrane proteins could therefore be in shielding the protein from the effects of fluctuations in bilayer thickness resulting from thermal motion in the fluid, liquid-crystalline state.

ACKNOWLEDGMENT

We thank Professor James Bowie for the generous gift of the clone for DGK.

REFERENCES

1. Lee, A. G. (2003) *Biochim. Biophys. Acta 1612*, 1−40.
2. Landolt-Marticorena, C., Williams, K. A., Deber, C. M., and Reithmeier, R. A. F. (1993) *J. Mol. Biol. 229*, 602−608.
3. Ulmschneider, M. D., and Sansom, M. S. P. (2001) *Biochim. Biophys. Acta 1512*, 1−14.
4. Braun, P., and von Heijne, G. (1999) *Biochemistry 38*, 9778−9782.
5. Lakowicz, J. R. (1999) *Principles of Fluorescence Spectroscopy*, Kluwer Academic/Plenum Press, New York.
6. Badola, P., and Sanders, C. R. (1997) *J. Biol. Chem. 272*, 24176−24182.
7. Walsh, J. P., and Bell, R. M. (1986) *J. Biol. Chem. 261*, 6239−6247.
8. Lau, F. W., Chen, X., and Bowie, J. U. (1999) *Biochemistry 38*, 5521−5527.
9. Smith, R. L., O'Toole, J. F., Maguire, M. E., and Sanders, C. R. (1994) *J. Bacteriol. 176*, 5459−5465.
10. Pilot, J. D., East, J. M., and Lee, A. G. (2001) *Biochemistry 40*, 8188−8195.
11. Pilot, J. D., East, J. M., and Lee, A. G. (2001) *Biochemistry 40*, 14891−14897.
12. Czerski, L., and Sanders, C. R. (2000) *FEBS Lett. 472*, 225−229.
13. East, J. M., and Lee, A. G. (1982) *Biohemistry 21*, 4144−4151.
14. Rooney, E. K., and Lee, A. G. (1986) *J. Biochem. Biophys. Methods 120*, 175−189.
15. Lau, F. W., and Bowie, J. U. (1997) *Biochemistry 36*, 5884−5892.
16. Ladokhin, A. S., Jayasinghe, S., and White, S. H. (2000) *Anal. Biochem. 285*, 235−245.
17. Caputo, G. A., and London, E. (2003) *Biochemistry 42*, 3265−3274.
18. Bolen, E. J., and Holloway, P. W. (1990) *Biochemistry 29*, 9638−9643.
19. Ladokhin, A. S. (1999) *Biophys. J.* 76, 946−955.
20. Koppel, D. E., Fleming, P. J., and Strittmatter, P. (1979) *Biochemistry 18*, 5450−5457.
21. Abrams, F. S., and London, E. (1992) *Biochemistry 31*, 5312−5322.
22. Mall, S., Broadbridge, R., Sharma, R. P., East, J. M., and Lee, A. G. (2001) *Biochemistry 40*, 12379−12386.
23. Lewis, B. A., and Engelman, D. M. (1983) *J. Mol. Biol. 166*, 211−217.
24. Lau, F. W., Nauli, S., Zhou, Y., and Bowie, J. U. (1999) *J. Mol. Biol. 290*, 559−564.
25. Wen, J. A., Chen, X., and Bowie, J. U. (1996) *Nat. Struct. Biol. 3*, 141−148.
26. Kaneko, T., Tanaka, A., Sato, S., Kotani, H., Sazuka, T., Miyajima, N., Sugiura, M., and Tabata, S. (1995) *DNA Res. 2*, 153−166.
27. Oxenoid, K., Sonnichsen, F. D., and Sanders, C. R. (2002) *Biochemistry 41*, 12876−12882.
28. Toyoshima, C., Nakasako, M., Nomura, H., and Ogawa, H. (2000) *Nature 405*, 647−655.
29. Williamson, I. M., Alvis, S. J., East, J. M., and Lee, A. G. (2002) *Biophys. J. 83*, 2026−2038.

BI034607E